

Supporting Information

High-density reconstitution of functional water channels into vesicular and planar block copolymer membranes

Manish Kumar, Joachim E. O. Habel, Yue-xiao Shen,
Wolfgang P. Meier, and Thomas Walz

MATERIALS AND METHODS

Polymers. PMOXA-PDMS-PMOXA polymers were synthesized as in Ref. 1 with the modifications described in Ref. 2. PB-PEO polymers were obtained from Polymer Source Inc., Canada. DOPE was purchased from Avanti Polar Lipids, Alabaster, AL.

Protein purification. AQP0 was purified from sheep eye lenses as described³ **Reconstitution of AQP0 into BCP membranes.** 10 mg of BCPs were dissolved in 2 ml chloroform, which was first evaporated under a stream of argon or nitrogen to form a thin film on the wall of a glass vial. Residual chloroform was removed by placing the vial in vacuum for 2-3 hours. To obtain a solution of BCP in 10% OG, 100 mg of solid OG was placed in a vial and 0.01% NaN₃ solution was added to a volume of 1 ml. The sample was stirred overnight, and, if the solution remained turbid, sonication was used to dissolve residual BCPs. The sample was finally filtered through a 0.2 µm track-etched Nucleopore filter and stored at 4°C.

To prepare dialysis samples, purified AQP0 (for a final concentration of 1 or 1.5 mg/ml) was mixed with OG-solubilized BCPs to obtain the desired PoPR (ranging from 250 to 0.1), and the sample volume was adjusted to 60 µl with detergent-containing dialysis buffer. After placing the dialysis sample into a 50-µl dialysis button (model HR3-326, Hampton research, Aliso Viejo,

CA), the button was sealed with dialysis tubing (Spectrapor -12-14 kDa) and placed into dialysis buffer.

Several dialysis conditions were tested to incorporate AQP0 into BCP membranes, including dialysis temperatures of 37°C, room temperature, and 4°C. Various compositions of the reconstitution buffer were screened, but the best results were obtained with 10 mM MES, pH 6, 100 mM NaCl, 50 mM MgCl₂, and 0.01% NaN₃, the buffer previously used to reconstitute AQP0 into lipid membranes.^{3,4} The detergent removal rate during dialysis was also varied by including detergent in the initial dialysis buffer, which was gradually reduced by dilution with detergent-free buffer (see Supplementary Figure 4 for details). The best conditions for reproducible incorporation of AQP0 into BCP membranes were dialysis at 4°C and an initial OG concentration in the dialysis buffer (50 ml) of 4%, which was halved every 12 hours by doubling the dialysis buffer volume with detergent-free buffer until the OG concentration reached 0.25% on the 4th day. On the 5th day the dialysis buffer was exchanged 3 times every 4 hours with detergent-free buffer, and the buttons were then harvested. This protocol ensured a low detergent removal rate of ~5.1 mg/ml/day (mg detergent/ml sample/days of dialysis). To test the effect of a moderate detergent removal rate, buttons were dialyzed for the 1st day against 0.1% OG dialysis buffer, and from the 2nd day on against detergent-free dialysis buffer. To test the effect of a high detergent removal rate, buttons were dialyzed for the 1st day against dialysis buffer containing 2% OG. On the 2nd day, the OG concentration in the dialysis buffer was lowered to 0.1% OG, and from the 3rd day on, OG was omitted from the dialysis buffer. Although these protocols appear counterintuitive, three repetitions of these protocols yielded reproducible detergent removal rates of ~14.6 mg/ml/day for the moderately fast detergent removal protocol, and ~19.4 mg/ml/day for the fast detergent removal protocol.

Determining the detergent concentration and its reduction during dialysis. To determine the detergent concentration and to follow its reduction during the dialysis process, a contact angle method was used.⁵ In this method, the contact angle of a detergent solution on a standard surface is measured. To relate the contact angle to the detergent concentration, a calibration curve is used that is obtained with buffer solutions containing known detergent concentrations. To generate the calibration curve, AQP0-PB12 vesicles (PoPR15) were prepared using the slow dialysis method described above, followed by an additional three days of dialysis against detergent-free buffer. An excess of polystyrene hydrophobic detergent absorption beads, Biobeads® (capable of removing 10x the initial detergent concentration in the dialysis buttons) was added to the dialysis buffer during the final three days of dialysis to ensure that no significant amount of detergent remained in the dialysis buffer. After harvesting the vesicles, various amounts of OG were added to the vesicles, and these solutions were used to measure the contact angles. Supplementary Figure S2 shows the calibration curve obtained for the AQP0/PB12/OG system. For OG concentrations higher than its critical micelle concentration, cmc (~0.7%), the detergent concentration was determined by first diluting the samples with detergent-free buffer.

To follow the removal of detergent by dialysis, buttons were prepared with 60 µl of a solution containing 1 mg/ml AQP0, 0.58 mg/ml PB12 (PoPR of 15) and 3.8% OG. The buttons were then dialyzed using the protocols described above. At various time points during the dialysis, buttons were harvested, and the contact angle of a 10-µl sample was measured, which was converted to the detergent concentration using the calibration curve shown in Supplementary Figure S2. The reduction in detergent concentration over time using the standard slow dialysis protocol is shown in Supplementary Figure S3.

Electron microscopy and image processing. BCP–protein aggregate samples were diluted 10 to 100 times with the dialysis buffer used to produce the aggregates. A 3.5- μ l sample was applied to a glow-discharged, carbon-coated copper EM grid and negatively stained with 0.75% uranyl formate as described.⁶ Images were recorded with a Phillips CM10 electron microscope at an acceleration voltage of 100 kV. Images were taken at a magnification of either 5200x or 52,000x on a 1K \times 1K CCD camera (Gatan). Lattice unbending and Fourier transformation were performed with the 2dx software.⁷

Water permeability measurements. To study the water permeability of BCP–AQP0 vesicles, AQP0 was reconstituted with PB12 at a PoPR of 15. The buffer used for dialysis was 10 mM MES, pH 6.5, 100 mM NaCl, 50 mM MgCl₂, and 0.01% NaN₃. After dialysis, the vesicles were extruded 20 times using 0.2 μ m track-etched Nucleopore filters to form unilamellar vesicles and characterized by EM and dynamic light scattering.

Control PB12 vesicles were synthesized using a previously reported method.⁸ A stock solution of 100 to 500 ml 10 mg/ml PB12 polymer in chloroform was placed into a glass vial, and the chloroform was evaporated in a stream of argon gas while rotating the glass vial to form a thin film. Traces of solvent were removed by placing the vial under vacuum for a minimum of 2 hours. Reconstitution buffer (the same buffer as used for reconstitution of AQP0) with 100 mM sucrose was then added to this film, and the glass vial was gently shaken. Vesicles formed within an hour and were characterized by EM and dynamic light scattering.

The water permeability of PB12 and PB12–AQP0 vesicles was measured by following the light scattering with a SF-E100 stopped-flow device from KinTek Corporation, Austin, TX. A 300 mOsm sucrose solution was used for pure PB12 vesicles and a 50 mOsm sucrose solution for PB12–AQP0 vesicles. The sucrose was added to the buffers in which the vesicles were

formed. Experiments were performed with three independent vesicle preparations to ensure reproducibility. A minimum of 10 traces were averaged for each experimental condition. Vesicle size was measured using a Viscotek TDA Model 302 dynamic light scattering device, and water permeability was calculated as described.⁸

To test the effect of residual detergent on membrane permeability, detergent-free PB12 vesicles were prepared as described above for the determination of the contact angle calibration curve. Various amounts of OG were added to these vesicles, and the samples were used to measure the water permeability of the vesicles. Detergent concentrations up to 0.01% had no measurable effect on the water permeability of the PB12 vesicles (Supplementary Figure S7).

CALCULATIONS

Calculating the hydrophilic volume ratio of BCPs

The hydrophilic volume ratio was calculated using a procedure similar to that used in Supplementary Ref. 9. The molecular mass of the synthesized hydrophilic or hydrophobic block was converted to molecular volume by using the density of the BCP hydrophobic and hydrophilic blocks for pure homopolymers of similar MW obtained from manufacturer's data (Sigma Aldrich). The hydrophilic volume ratio was then calculated by dividing the volume of the hydrophilic block by the sum of the volumes of the hydrophilic and hydrophobic blocks. The densities used and an example for each type of polymer are shown below:

	Dp	MW g/mol	mass g	density g/cm ³	volume cm ³	f _{hydrophilic}
PB-PEO						
PB	22	54.1	1.98 x 10 ⁻²¹	0.86	2.30 x 10 ⁻²¹	0.28
PEO	14	44	1.02 x 10 ⁻²¹	1.13	9.05 x 10 ⁻²²	
PDMS-PMOXA						
PDMS	42	74	5.16 x 10 ⁻²¹	0.97	5.32 x 10 ⁻²¹	0.51
PMOXA	20	85	2.82 x 10 ⁻²¹	1	2.82 x 10 ⁻²¹	

Dp: degree of polymerization (number of repeat units per block)

Calculating the hydrophilic volume ratio of DOPE

The hydrophobic and hydrophilic volumes for DOPE were estimated from the mean molecular area of the lipid in a bilayer (65.8 Å²; Supplementary Ref. 10) and the average position of the hydrophobic/hydrophilic boundary in the hydrated structure of a similar lipid, 1,2-dioleoyl-sn-glycero-3-phosphocholine (DOPC), described in simulations.¹⁰ The total length of the lipid molecule in this model is 19.8 Å, and the length of the hydrophobic chains up to the position of the phosphate group is 16.0 Å. The volumes approximated with these values are 1.05 x 10⁻²¹ cm³ for the hydrophobic part and 2.52 x 10⁻²² cm³ for the hydrophilic part of the lipid. The total DOPE volume is thus 1.30 x 10⁻²¹ cm³ and the hydrophilic volume ratio of DOPE comes to 0.24.

Calculating the volume fraction of AQP0 in BCP–protein and lipid–protein aggregates

We determined the total, hydrophobic, and hydrophilic volumes of AQP0 from its atomic structure,² using the program Open Structure.¹¹ The total volume was estimated as 2.89×10^{-20} cm³, and the hydrophobic and hydrophilic volumes as 1.89×10^{-20} cm³ and 9.96×10^{-21} cm³, respectively.

The volume fraction of AQP0 (f_{AQP0}) in polymer–protein and lipid–protein aggregates was calculated using the hydrophobic volume of AQP0 and the volumes of the polymers or lipid. First, the molar PoPR or LPR was used to calculate the number of AQP0 molecules (for PoPR or LPR > 1) or the fraction of an AQP0 molecule (for PoPR or LPR < 1) associated with one polymer or lipid molecule in the aggregate. This number was multiplied with the hydrophobic volume of AQP0 to obtain the hydrophobic volume of AQP0 in an aggregate unit. The total volume of the aggregate unit was then calculated as the sum of the volume of the polymer or lipid added to the hydrophobic AQP0 volume in the aggregate unit. The volume fraction of AQP0 in an aggregate is the hydrophobic AQP0 volume in the aggregate unit divided by the total volume of the aggregate unit.

TABLES

Table S1: Molar LPRs for various aquaporin 2D crystals in lipid membranes

Protein	Lipid	LPR	AQP		mLPR	Reference
		(w/w)	MW	Lipid MW		
AQP0	DOPE	0.35	28121	744.0	13.2	this study
AQP0	EPL	0.25	28121	798.0	8.8	Hite et al, 2010 ⁴
AQP0	DMPC	0.25	28121	677.9	10.4	Gonen et al, 2005 ³
AqpZ	DMPC/POPC	0.35	23702	719.0	11.5	Ringler et al, 1999 ¹²
AQP1	EPL	0.5	28526	798.0	17.9	Walz et al, 1994 ¹³
AQP9	DMPC	0.5	31871	677.9	23.5	Viadiu et al, 2007 ¹⁴
AQP2	EPL	0.5	28837	798.0	18.1	Schenk et al, 2005 ¹⁵
AQP4	EPL	1	34480	798.0	43.2	Hiroaki et al, 2006 ¹⁶

DOPE: 1,2-dioleoyl-sn-glycero-3-phosphoethanolamine, EPL: *E. coli* polar lipids, DMPC: 1,2-dimyristoyl-sn-glycero-3-phosphocholine, POPC: 1-palmitoyl-2-oleoyl-sn-glycero-3-phosphocholine.

Table S2: Morphological transitions of BCP and DOPE membranes with increasing AQP0 concentrations

mPoPR	Morphology	mPoPR	Morphology	mPoPR	Morphology
PB12		ABA42		DOPE	
∞ (no protein)	N	∞ (no protein)	V	∞ (no protein)	V
258.2	N/V	43.2	V	200	V
51	V	25.9	V	50	V
25.82	V	8.6	V	14.2	M
15.49	V	4.3	V/M	13.3	M
7.75	V	2.6	V/M	12.5	C
6.45	V	2.2	M		
3.87	M	0.9	M		
2.6	M	0.6	C		
1.29	C	0.2	C		
0.52	C				
PB22		ABA55			
∞ (no protein)	N	∞ (no protein)	V		
778.49	V	46	V		
311.39	V	27.6	V		
155.7	V	9.2	V/M		
31.14	V/M	2.8	M		
15.57	V/M	1.5	M		
9.34	M/V				
7.79	M/V				
3.11	M				
1.56	M				
0.78	M				
0.39	M				

N: native structures; V: vesicles; M: planar membranes; C: 2D crystals

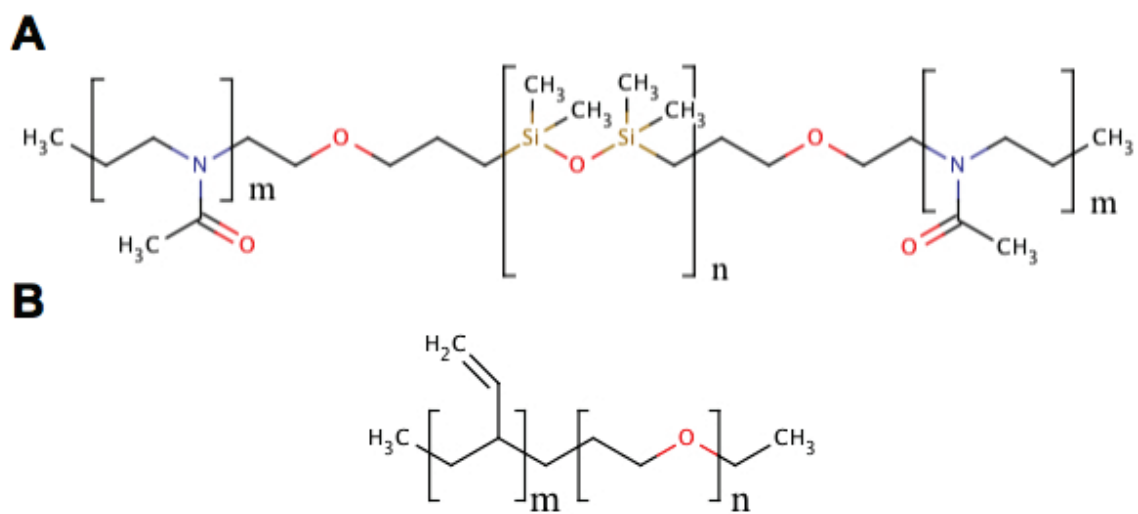


Figure S1: Polymer structures. A. PMOXA-PDMS-PMOXA. B. PEO-PB.

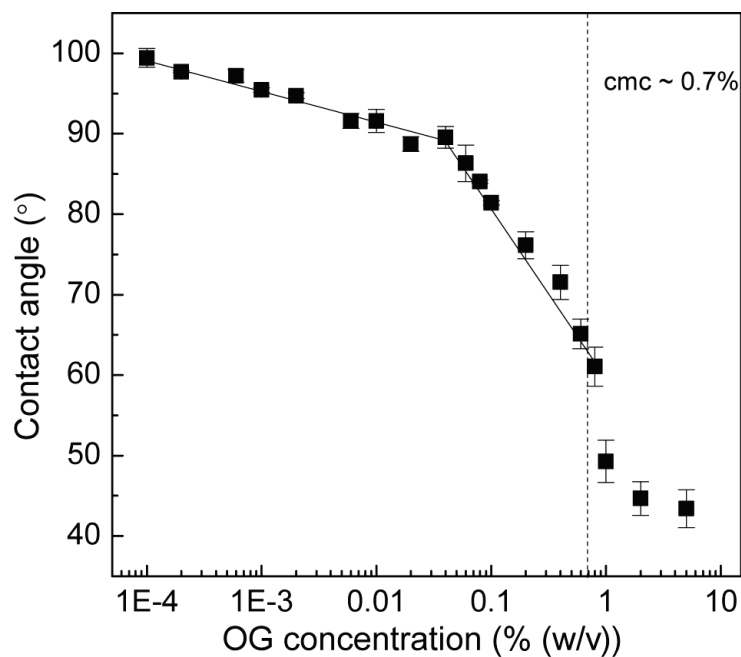


Figure S2: Calibration curve determined with PB12 vesicle solutions containing known OG concentrations and used to convert measured contact angles to OG concentrations. The contact angle method can only be used to measure the concentration of a detergent below its cmc ($\sim 0.7\%$ for OG). Detergent concentrations above the cmc were therefore measured by first diluting the sample with detergent-free buffer.

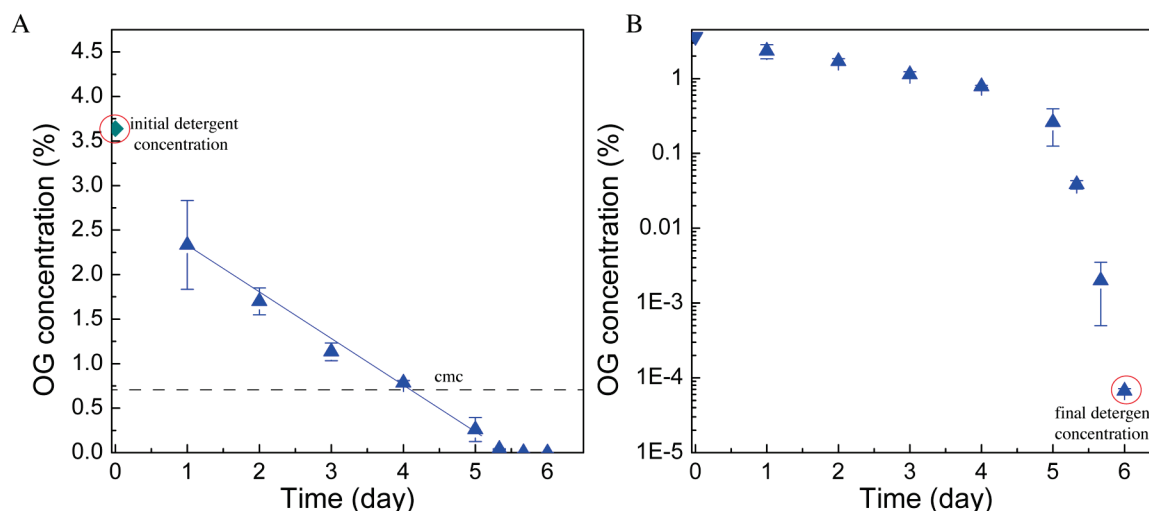


Figure S3: Detergent removal over time by using the standard slow dialysis protocol. A. The initial detergent concentration was measured as 3.7% (red circle). The slope of the blue line represents the detergent removal rate when the system passes through the cmc of the detergent (OG; $\sim 0.7\%$). As the concentration of the detergent solubilizing the protein and the polymer approaches its cmc, a transition is expected to occur from mixed micelles to higher-order structures such as vesicles. The detergent removal rate during this transition was used to describe the characteristic detergent removal rate for a given dialysis procedure. This choice is relevant to the current study, because the transition region in which mixed micelles begin to convert to higher-order structures has been shown to affect the morphology of the resulting aggregates.¹⁷ With the slow detergent removal protocol, the rate was 5.1 mg/ml/day. B. Same data as in A shown on a log scale to highlight the final detergent concentration at the end of the dialysis procedure used, which was $\sim 0.0001\%$ (red circle).

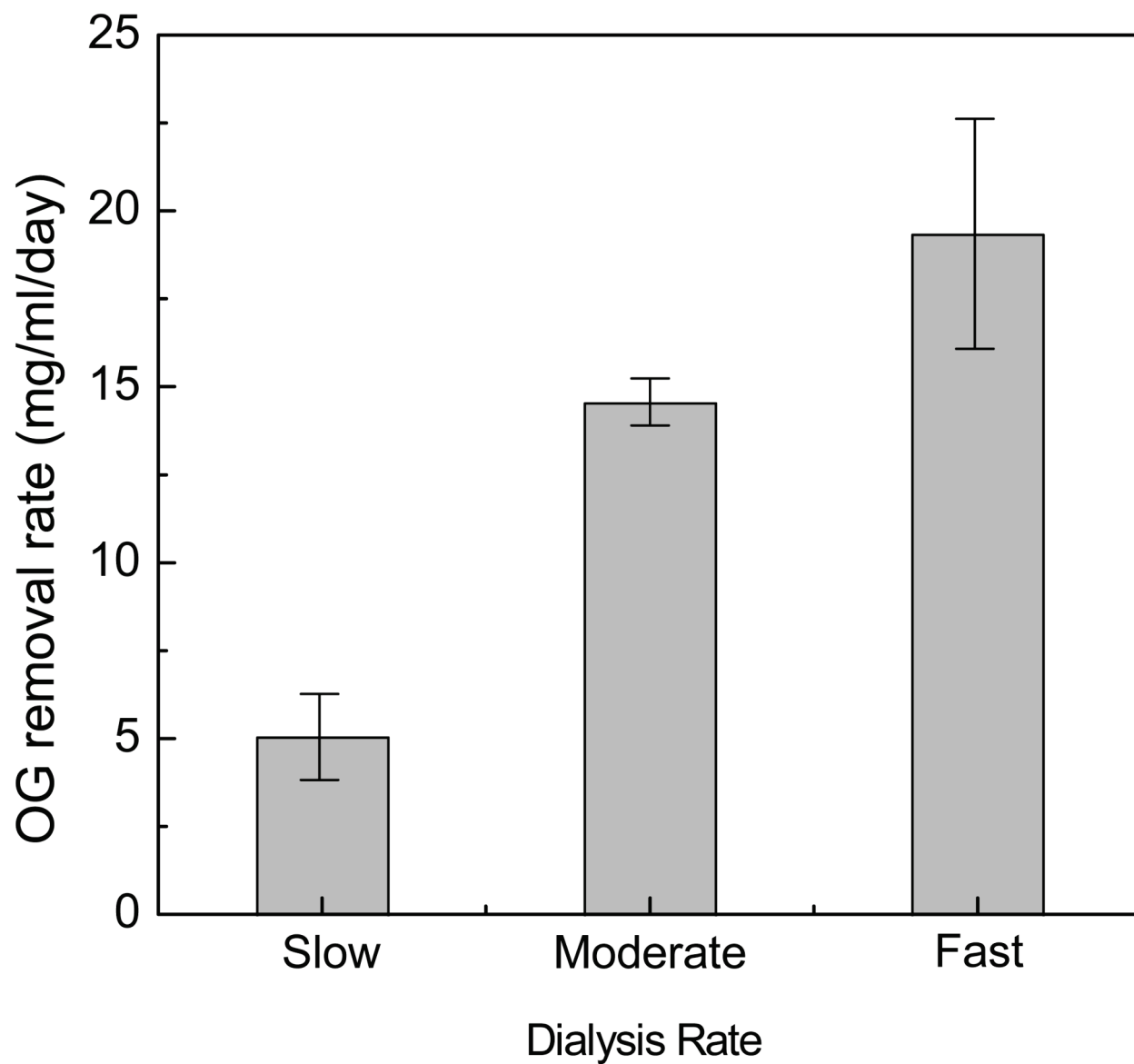


Figure S4: The critical detergent removal rates, defined as the detergent removal rate as the system transitions through the cmc of the detergent, for the three used protocols were 5.1 mg/ml/day for slow dialysis, 14.6 mg/ml/day for moderately fast dialysis and 19.4 mg/ml/day for fast dialysis. All dialyses were conducted at 4°C.

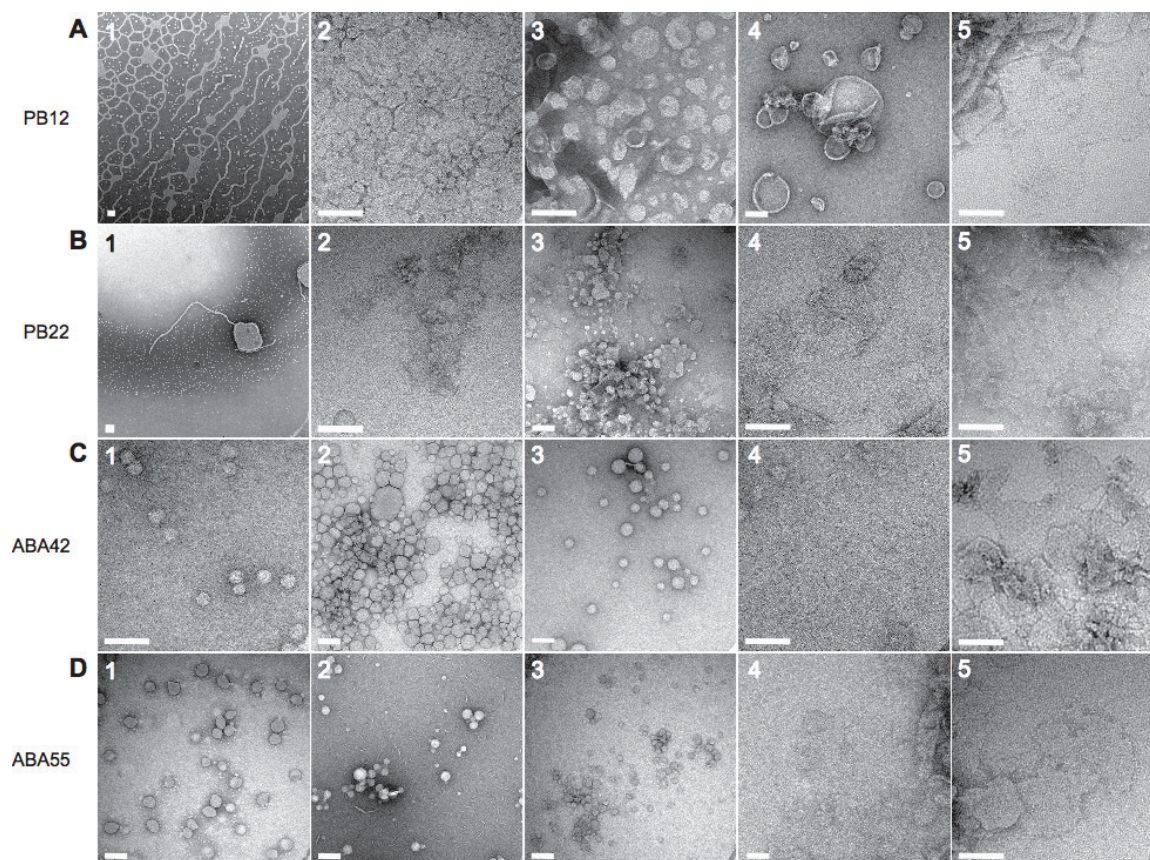


Figure S5: Effect of increasing protein concentrations (decreasing PoPRs) on aggregate morphology for all block copolymers tested. The micrographs show PoPRs that are representative of the range in which a particular aggregate morphology is dominant. A. Reconstitution of AQP0 with PB12 at molar PoPRs of (1) ∞ (no protein), (2) 258, (3) 51, (4) 15.5, and (5) 1.3. The increase in incorporated protein leads to a transition from the network structures formed by pure polymer described before,¹⁸ to a mixture of network structures and vesicles, to vesicles only, and finally to crystalline membrane patches. B. Reconstitution of AQP0 with PB22 at PoPRs of (1) ∞ (no protein), (2) 156, (3) 31, (4) 9.3, and (5) 1.6. With increasing protein incorporation, the aggregates transition from a mixture of small vesicles and vesicles with attached tubes, to a mixture of membrane patches and vesicles, and finally to membrane patches only. C. Reconstitution of AQP0 with ABA42 at PoPRs of (1) ∞ (no protein), (2) 43.2, (3) 8.6, (4) 2.2, and (5) 0.6. The aggregates transition from vesicles only, to a

mixture of membrane patches and vesicles, to membrane patches only, and finally to crystalline membrane patches. D. Reconstitution of AQP0 with ABA55 at PoPRs of (1) ∞ (no protein), (2) 46, (3), 9.2, (4) 2.8, and (5) 1.5. There is a transition from vesicles only to a mixture of membrane patches and vesicles, to membrane patches only. All scale bars are 100 nm.

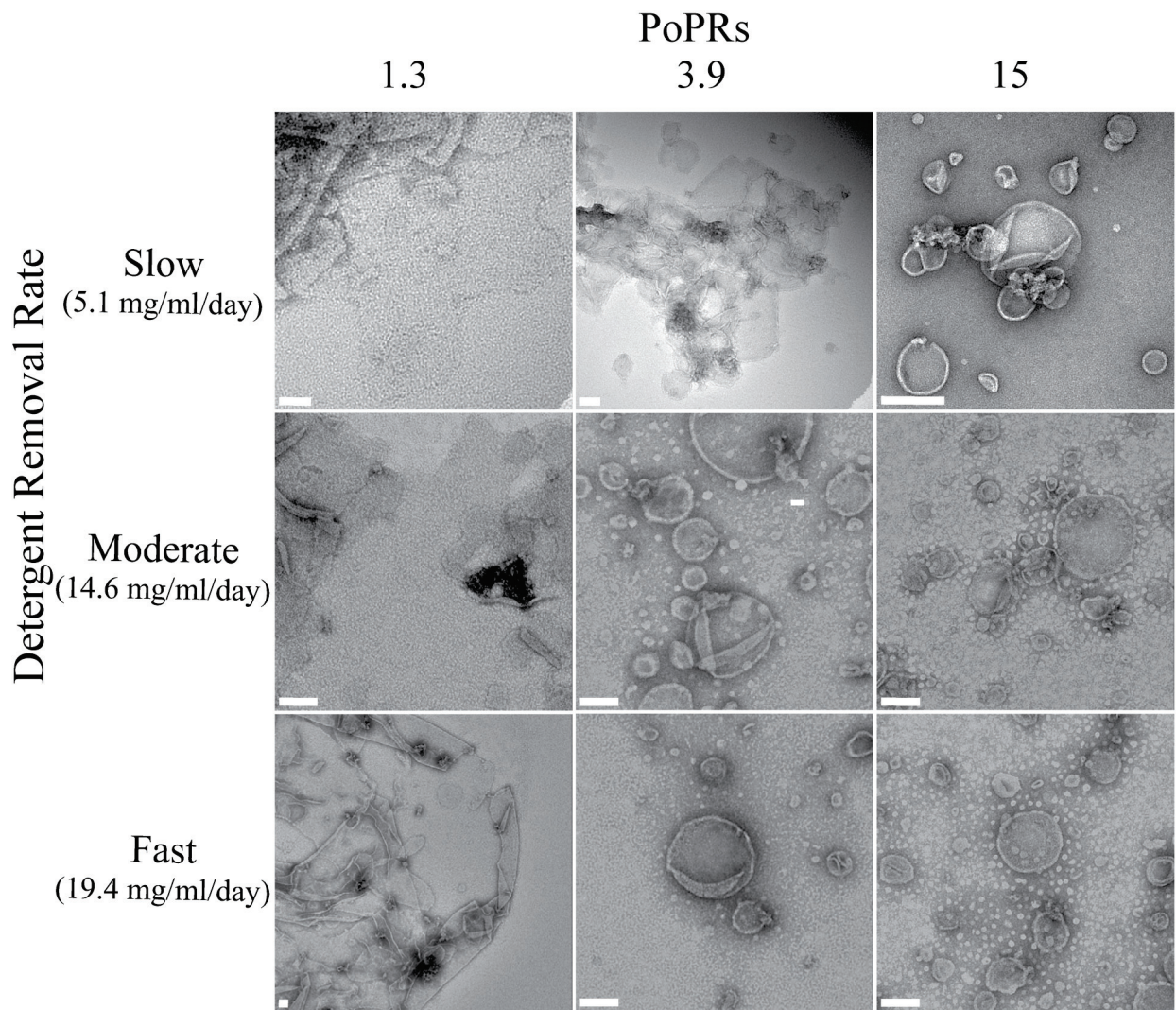


Figure S6: Effect of detergent removal kinetics on PB12–AQP0 aggregate morphology. Compared to the variety of aggregate morphologies that formed at the low dialysis rate (2D crystals, planar membrane sheets, and vesicles), higher dialysis rates resulted in a preponderance of vesicular structures. In contrast to the slow dialysis protocol, the faster dialysis protocols also resulted in a substantial background of small polymer vesicles or micelles potentially containing AQP0 (white spots in images), indicating a decrease in efficient incorporation of AQP0 into extended PB12 membranes. With the moderate dialysis rate and the low PoPR of 1.3 (at which AQP0 formed 2D crystals with the low dialysis rate), large planar membranes and several collapsed vesicles were seen, which occasionally contained poorly ordered 2D arrays of AQP0.

At a PoPR of 3.9, large, non-crystalline vesicles formed, and at a PoPR of 15, again vesicles formed with some small polymer micelles or vesicles visible in the background. With the high dialysis rates, the vesicle size increased with decreasing PoPRs, similar to the tendency seen with the low dialysis rate. In particular, at the lowest PoPR of 1.3, large, folded membranes formed (non-crystalline), while at higher PoPRs smaller vesicles formed with a large quantity of small polymer vesicles or micelles seen in the background (white spots on images). Scale bars are 100 nm.

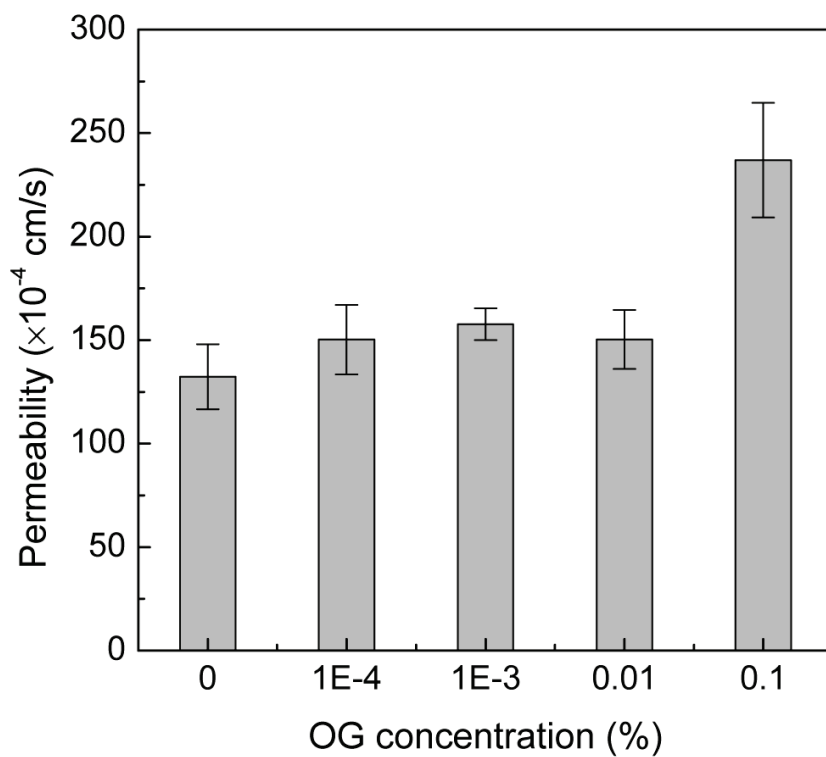


Figure S7: Effect of detergent concentration on the water permeability of pure PB12 polymer vesicles. Up to an OG concentration of 0.01%, the measured water permeability was not significantly different from the one in the absence of detergent. At an OG concentration of 0.1%, the measured water permeability increased by 79%.

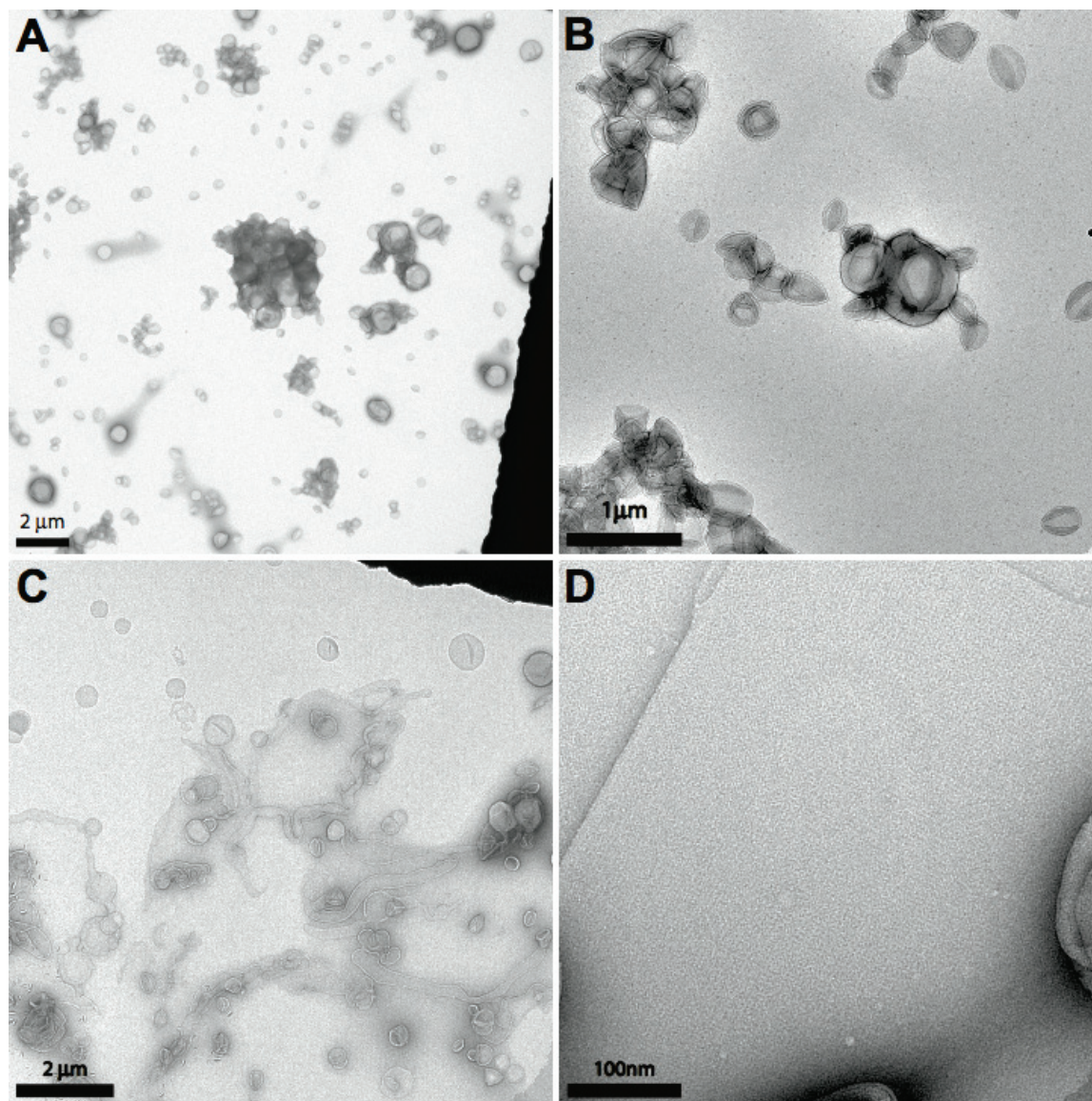


Figure S8: Morphological transition of DOPE membranes with increasing AQP0 concentrations.

A. In the absence of protein, DOPE forms vesicles. B. At a molar LPR of 50, the membranes remain vesicular but increase in size. C. At a molar LPR of 13.3, planar membranes begin to form. D. At a molar LPR of 12.5, AQP0 forms crystalline arrays in planar DOPE membranes.

References

- (1) Nardin, C.; Hirt, T.; Leukel, J.; Meier, W. *Langmuir* **2000**, *16*, 1035–1041.
- (2) Kumar, M.; Grzelakowski, M.; Zilles, J.; Clark, M.; Meier, W. *Proc Natl Acad Sci USA* **2007**, *104*, 20719–20724.
- (3) Gonen, T.; Cheng, Y.; Sliz, P.; Hiroaki, Y.; Fujiyoshi, Y.; Harrison, S. C.; Walz, T. *Nature* **2005**, *438*, 633–638.
- (4) Hite, R. K.; Li, Z.; Walz, T. *EMBO J* **2010**, *29*, 1652–1658.
- (5) Kaufmann, T. C.; Engel, A.; Rémygy, H.-W. *Biophys J* **2006**, *90*, 310–317.
- (6) Ohi, M.; Li, Y.; Cheng, Y.; Walz, T. *Biol Proced Online* **2004**, *6*, 23–34.
- (7) Gipson, B.; Zeng, X.; Zhang, Z. Y.; Stahlberg, H. *J Struct Biol* **2007**, *157*, 64–72.
- (8) Discher, B.; Won, Y.; Ege, D.; Lee, J.; Bates, F.; Discher, D.; Hammer, D. *Science* **1999**, *284*, 1143–1146.
- (9) Schlaad, H.; Kukulka, H.; Smarsly, B.; Antonietti, M.; Pakula, T. *Polymer* **2002**, *43*, 5321–5328.
- (10) Mashl, R. J.; Scott, H. L.; Subramaniam, S.; Jakobsson, E. *Biophys J* **2001**, *81*, 3005–3015.
- (11) Biasini, M.; Mariani, V.; Haas, J.; Scheuber, S.; Schenk, A. D.; Schwede, T.; Philippsen, A. *Bioinformatics* **2010**, *26*, 2626–2628.
- (12) Ringler, P.; Borgnia, M.; Stahlberg, H.; Maloney, P.; Agre, P.; Engel, A. *J Mol Biol* **1999**, *291*, 1181–1190.
- (13) Walz, T.; Smith, B. L.; Zeidel, M. L.; Engel, A.; Agre, P. *J Biol. Chem.* **1994**, *269*, 1583–1586.
- (14) Viadiu, H.; Gonen, T.; Walz, T. *J Mol Biol* **2007**, *367*, 80–88.

- (15) Schenk, A.; Werten, P.; Scheuring, S.; de Groot, B.; Muller, S.; Stahlberg, H.; Philippsen, A.; Engel, A. *J Mol Biol* **2005**, *350*, 278–289.
- (16) Hiroaki, Y.; Tani, K.; Kamegawa, A.; Gyobu, N.; Nishikawa, K.; Suzuki, H.; Walz, T.; Sasaki, S.; Mitsuoka, K.; Kimura, K. *J Mol Biol* **2006**, *355*, 628–639.
- (17) Dolder, M.; Engel, A.; Zulauf, M. *FEBS Letters* **1996**, *382*, 203–208.
- (18) Jain, S.; Bates, F. *Science* **2003**, *300*, 460–464.